Chinese Chemical Letters 35 (2024) 109725

Contents lists available at ScienceDirect

Chinese Chemical Letters

journal homepage: www.elsevier.com/locate/cclet

Augmenting levoglucosan production through catalytic pyrolysis of biomass exploiting $Ti_3C_2T_x$ MXene

Junqi Wang[a,*], Shuai Zhang[a], Jingjing Ma[a], Xiangjun Liu[a], Yayun Ma[b], Zhimin Fan[c,*], Jingfeng Wang[d,*]

[a] School of Human Settlements and Civil Engineering, Xi'an Jiaotong University, Xi'an 710049, China
[b] Core Facilities and Experiment Center of Xi'an Jiaotong University, Xi'an Jiaotong University, Xi'an 710049, China
[c] MIIT Key Laboratory of Critical Materials Technology for New Energy Conversion and Storage, School of Chemistry and Chemical Engineering, Harbin Institute of Technology, Harbin 150001, China
[d] Advanced Materials Research Central, Northwest Institute for Nonferrous Metal Research, Xi'an 710016, China

ARTICLE INFO

Article history:
Received 22 November 2023
Revised 19 February 2024
Accepted 5 March 2024
Available online 6 March 2024

Keywords:
Levoglucosan
$Ti_3C_2T_x$ MXene
Catalytic pyrolysis
Py-GC/MS
Lab-scale

ABSTRACT

To address the pressing global need for carbon-neutral fuels, optimizing the conversion of biomass to bio-oil (bio-chemicals) is crucial. Here, we introduce MXene ($Ti_3C_2T_x$) as an innovative catalyst in biomass pyrolysis, exhibiting significant prowess in boosting levoglucosan yields. Py-GC/MS analysis indicated a remarkable 438% enhancement in levoglucosan yield when a 5 wt% catalyst-to-biomass ratio was employed. Laboratory-scale studies achieved an impressive 13.95 wt% levoglucosan in *ex-situ* fixed-bed catalytic pyrolysis, a yield that is 19.6 times higher than that from pure biomass at 40 wt% catalyst loading. Recycling evaluations affirm the robust stability of the MXene catalyst, validating its potential for multiple use cycles in eco-friendly industrial levoglucosan production.

The escalating global dependence on fossil fuels has heightened environmental issues, emphasizing the need for carbon-neutral and low-emission fuels. Pyrolysis technology emerges as a promising method, rapidly converting biomass into bio-oil containing crucial chemicals, with levoglucosan being particularly noteworthy. Levoglucosan, also known as 1,6-Anhydro-β-D-glucopyranose, is a crucial industrial chemical primarily derived from petroleum sources [1]. It has been identified by the US Department of Energy as one of the most promising chemicals in the field of "sugar-based biorefinery" [2]. The applications of levoglucosan across diverse fields, serving as a valuable precursor for synthesizing organic acids, platform chemicals, and specialty chemicals [3,4]. Its potential applications extend to the pharmaceutical industry. Levoglucosan plays a pivotal role in producing flame-retardant materials, especially in textiles and polymers. Additionally, it contributes to the production of carbon materials utilized in energy storage devices. The broad spectrum of applications underscores levoglucosan significance in supporting various industries and sustainable technologies.

Thermal decomposition of cellulose is the way of levoglucosan production in biomass pyrolysis. However, the intricate interplay among biomass components complicates bio-oil composition, posing challenges for consistent high levoglucosan yields [5]. While researchers explore pretreatment strategies, such as acid and alkaline methods [6], to enhance levoglucosan output, these approaches often involve drawbacks, including waste generation and sustainability concerns. In contrast, catalyst-assisted pyrolysis offers selective conversion, simplified technology, and improved product formation in bio-oils, yet comprehensive research on levoglucosan synthesis through this method remains limited.

MXene, characterized by its 2D structure, high specific surface area, and abundant active sites, holds promise for various applications such as electrocatalysis, photocatalysis, and photoelectrocatalysis [7]. With its unique physicochemical properties, including a stable $M_{n+1}X_n$ skeleton and adjustable surface termination groups (•OH, •O, and •F), MXene may serve as a high-performance thermal catalyst, offering catalytic activity akin to noble metals and high thermal stability [8]. However, as of now, the utilization of MXene in pyrolysis remains unexplored.

This research aims to investigate the catalytic performance and recyclability of MXene ($Ti_3C_2T_x$) in enhancing levoglucosan yield through pyrolysis and catalytic upgrading experiments. Utilizing Py-GC/MS analysis and a lab-scale reactor for *in-situ* and *ex-situ*

* Corresponding authors.
E-mail addresses: wjq@xjtu.edu.cn (J. Wang), fanzm@hit.edu.cn (Z. Fan), wangjingfengf@163.com (J. Wang).

https://doi.org/10.1016/j.cclet.2024.109725
1001-8417/

catalytic pyrolysis tests, the study aims to provide insights into the biomass pyrolysis mechanism and contribute to the design of more efficient pyrolysis catalysts, thereby advancing biomass utilization as a renewable energy source.

Populus tomentosa served as the biomass feedstock, undergoing preparation involving washing, drying, grinding, and sieving to achieve a particle size of approximately 1 mm. The prepared material, stored in a hermetically sealed container, was analyzed for cellulose, hemicellulose, and lignin contents using the NREL analytical procedure. In this study, the cellulose, hemicellulose, and lignin contents exhibited of 42.2 wt%, 22.3 wt%, and 19.5 wt%.

MXene was prepared using an improved method called minimally intensive layer delamination (MILD) [9]. The specific procedure was as follows: the Ti_3AlC_2 MAX precursor underwent selective etching to remove the Al layer using an HCl/LiF mixture. In a polytetrafluoroethylene beaker, 4 g of LiF and 50 mL of 9 mol/L HCl were thoroughly mixed by magnetic stirring. Then, 2.5 g of Ti_3AlC_2 powder was added in small portions multiple times and continuously stirred at 35 °C for 24 h to ensure a sufficient reaction. Once the reaction was complete, the precipitate was washed with deionized water through centrifugation at 3500 rpm until the pH reached neutral. The precipitate was then added to 200 mL of deionized water and shaken appropriately. Afterward, the dispersion was centrifuged at 3500 rpm for 15 min, and the homogeneous monolayer MXene dispersion was collected.

To examine the morphology and specific surface area of the MXene sample, scanning electron microscopy (SEM, Hitachi SU800SEM instrument) and Brunner-Emmet-Teller measurements (BET, BELSORP-Max, Japan) were conducted. Transmission electron microscopy (TEM) utilizing a Tecnai G2 F30, FEI instrument was employed to investigate the nanosheet morphologies of the delaminated MXene. For TEM analysis, the MXene dispersion was first diluted and deposited onto ultra-thin holey carbon film TEM grids. After air drying, the MXene sample was ready for TEM examination. Atomic force microscopy (AFM) images of the MXene nanosheets were acquired in tapping mode using a Bruker Dimension Fastscan instrument. Thermogravimetric analysis (TGA) was performed using a TGAQ50 analyzer under a nitrogen atmosphere (30 mL/min), employing different ratios of MXene with biomass and biomass alone.

Pyrolysis experiments coupled with gas chromatography/mass spectrometry (Py-GC/MS) were carried out using a Pyro-probe 5200 CDS system connected to a 7890A gas chromatograph and a 5975C mass spectrometer (Agilent Technologies, SantaClara, CA, USA). Approximately 200–300 μg of feedstock, including 1 wt%, 3 wt%, and 5 wt% MXene solutions, were filled into a pyrolysis tube with quartz wool at both ends. The experimental conditions entailed a residence time of 20 s at 500 °C, with a heating rate of 1000 °C/s. Other parameters were set based on the methodology outlined in a previous study [10].

In-bed catalytic pyrolysis analysis was conducted through Py-GC/MS, and laboratory-scale *ex-situ* catalytic pyrolysis experiments were performed using two distinct approaches. The first method involved adding freeze-dried MXene particles (referred to as MXene (P)) to establish various catalyst-to-biomass ratios (0, 5 wt%, 10 wt%, 20 wt%, 30 wt%, 40 wt%, and 50 wt%). This ratio is calculated by the mass of the catalyst relative to the mass of the biomass. The second method employed a"box in" configuration, with the MXene catalyst enclosed within a box (referred to as in MXene (Box)). *Ex-situ* experiments were carried out at 540 °C under a N_2 atmosphere, with a heating rate of 5 °C/min, in a fixed-bed reactor as described in our publication [11].

The yields of bio-oil and biochar were directly determined by weight, while the gas yield was obtained through subtraction. Condensable liquid products were collected using a mixture of chloroform and methanol. The levoglucosan yield was quantified using gas chromatography (Shimadzu HS-10/GC-2010Pro) *via* the external standard method. The gas chromatography measurement followed the same procedure as outlined in pyrolysis experiments. Each experiment was repeated three times to ensure the reliability of the results.

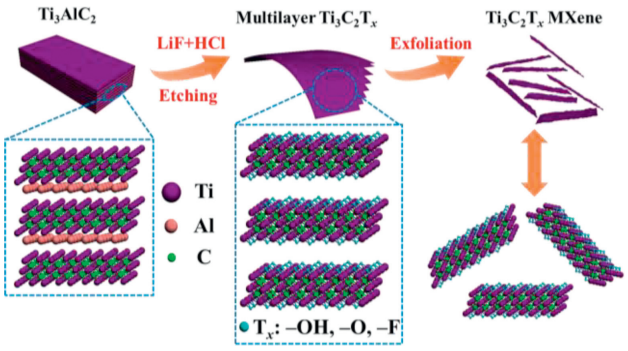

Fig. 1. Schematic depiction of the synthesis process for MXene.

Recycling experiments were conducted to evaluate the reusability and stability of the MXene catalyst using the laboratory-scale setup. For recycling, the pyrolyzed MXene (P) and biochar were easily separated and recovered from the pyrolytic solid residues *via* simple sieving. The pyrolyzed MXene (Box) could be reused by introducing fresh biomass. The catalytic pyrolysis of biomass was performed using the MXene (P_R and Box_R) catalyst in the recycling experiments. After each test, the used MXene (P_R and Box_R) was collected without any regeneration treatment and directly subjected to the subsequent recycling test. A total of five consecutive runs were performed, with the pyrolytic liquid obtained in each test being collected and analyzed.

Fig. 1 shows that Al layers were selectively removed from Ti_3AlC_2 through an etch and delamination process using HCl and LiF, resulting in MXene nanosheets. The concentrated dispersion of MXene exhibited a striking black hue, while its diluted counterpart displayed a captivating green color with a pronounced Tyndall effect (Fig. 2a). Subsequent characterization endeavors were undertaken to unravel the properties of the MXene flakes. A uniform distribution of titanium (Ti) elements (Fig. 2b) was discerned and the SEM findings showcase MXene nanosheets with a clean and smooth surface (Fig. 2c). In spite of the layered structure of multi-layer MXene becoming less evident after the etching process (Fig. 2d), a straightforward subsequent exfoliation process can readily produce single-layer MXene nanosheets. High-angle annular dark-field scanning transmission electron microscopy (HAADF-STEM) analysis (Fig. 2e) revealed that the lateral dimensions of the MXene flakes reached the micrometer scale, exhibiting a smooth surface devoid of noticeable signs of oxidation. Moreover, the BET surface area of MXene is 8.0284 m^2/g (Figs. 2f1 and f2), while the selected area exhibited distinct hexagonal lattice characteristics (Fig. 2g). AFM measurements indicate a thickness of approximately 1.5 nm (Fig. 2h). This thickness slightly exceeds the theoretical value, primarily due to factors like substrate roughness and the presence of MXene terminal groups. These findings affirm the successful preparation of low-defect, monolayer MXene with substantial dimensions in this experimental investigation. By subjecting the MXene dispersion to vacuum-assisted filtration, an MXene film was prepared, characterized by its delicate lavender texture on the surface (Fig. 2i).

To elucidate the impact of MXene addition on the pyrolysis behavior of biomass, thermogravimetry (TG) and differential thermogravimetry (DTG) were conducted. As illustrated in Fig. 3a, in the high-temperature region, the residual mass of biomass + MXene exceeded that of pure biomass, presumably owing to the excep-

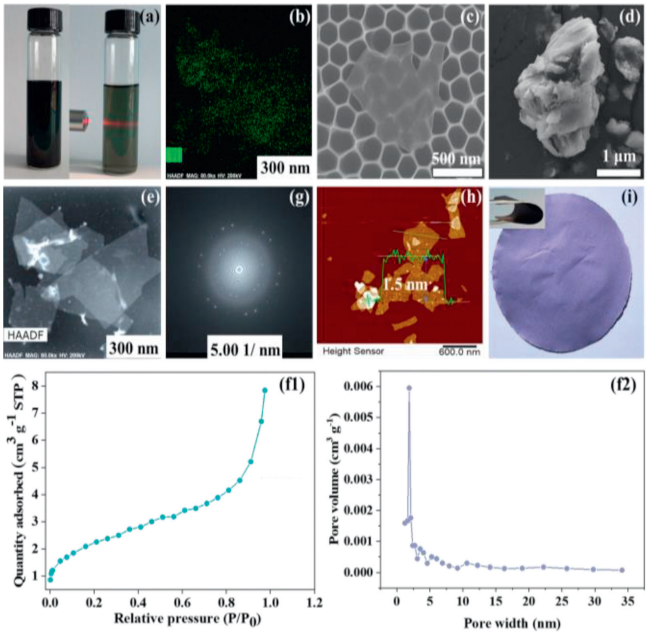

Fig. 2. (a) Concentrated dispersion of MXene and diluted dispersion of MXene with Tyndall effect. (b) Distribution of Ti in MXene flakes. (c) SEM imaging of MXene nanosheets supported on porous anodic aluminum oxide (AAO). (d) SEM image of multilayer MXene. (e) HAADF-STEM image of MXene flakes. (f1) N_2 adsorption isotherms of MXene. (f2) Pore size distribution of MXene. (g) Selected area diffraction of MXene flakes. (h) AFM image of MXene flakes. (i) Photographs of the MXene film, highlighting its remarkable flexibility in the inset.

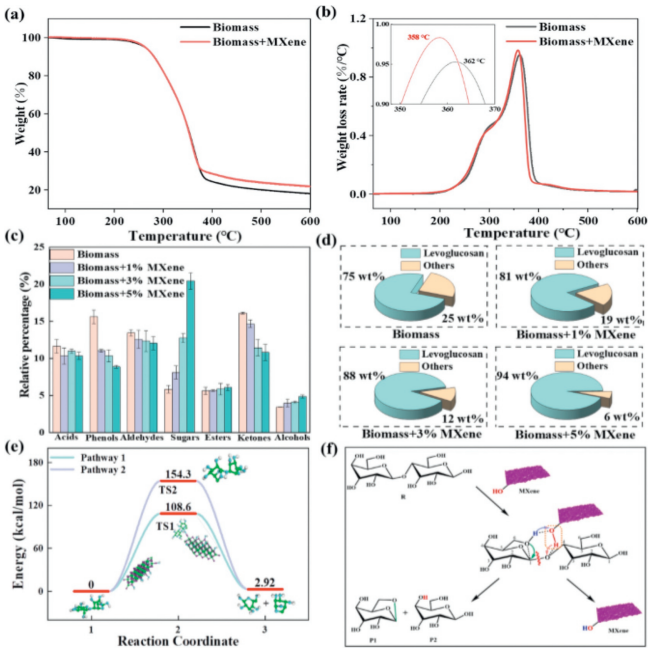

Fig. 3. (a) Thermogravimetry (TG) curves of biomass and biomass + MXene. (b) Differential thermogravimetry (DTG) curves of biomass and biomass + MXene. (c) Effect of different MXene loadings on bio-oil distribution during pyrolysis. (d) Effect of different MXene content on the distribution of LG and other sugars in pyrolysis. (e) Formation mechanism of LG and the associated potential energy. (f) Schematic diagram illustrating the influence of MXene on levoglucosan formation.

tional thermal stability conferred by MXene. The maximum degradation temperature of biomass was recorded as 362 °C, accompanied by a corresponding maximum degradation rate of 0.95% min^{-1} (Fig. 3b). The incorporation of MXene led to a reduction in the maximum degradation temperature to 358 °C, while concurrently enhancing the maximum degradation rate to 0.98% min^{-1}. This phenomenon can be attributed to the influence of MXene on the decomposition of hemicellulose, cellulose, and lignin, thereby expediting the pyrolysis of biomass and slightly reducing the pyrolysis temperature. It is worth noting that there is a "shoulder" peak in the DTG curves around 300 °C. This phenomenon is attributed to the cleavage of glycosidic bonds through the retro-Diels-Alder reaction following cellulose dehydration [12].

The composition of bio-oil, as revealed by Py-GC/MS experiments, is presented in Fig. 3c, namely acids, phenols, aldehydes, ketones, and sugars. Levoglucosan is a major constituent of sugars, primarily obtained through the pyrolysis of cellulose [13]. In this study, the content of levoglucosan in the bio-oil, in the absence of any catalyst, was a mere 4.39 wt% (Figs. 3c and d). However, when MXene was employed as a catalyst, the yield of levoglucosan significantly increased to 19.25 wt%, accompanied by a substantial reduction in the contents of other competing products (Figs. 3c and d). Apart from sugars, there was a slight increase in the content of alcohols, which may be attributed to MXene assisting in the secondary reactions of various volatile intermediates. These intermediates undergo secondary reactions, including dehydration, decarbonylation, and decarboxylation, ultimately resulting in the production of alcohols.

To explore the role of MXene in catalytic pyrolysis of cellulose into levoglucosan, Material Studio software is conducted. First, unrestricted geometric optimization is performed on all initial guess structures to find the minimum point of the system potential surface. All energies in the study are corrected for zero-point energy, the Slater-Koster library is selected as tiorg, and then the density functional theory B+ calculation method is used to estimate the reaction potential barrier by calculating the relative energy difference between the transition state and the reactants. In previous calculation models [14], the lowest energy pathway for cellulose pyrolysis reactions was through the formation of a four-membered ring transition state, which then generated levoglucosan.

However, based on our experimental findings, we hypothesize that when MXene is present, the generation pathway changes, leading to the formation of a six-membered ring. Compared to the four-membered ring TS1 (154.3 kcal/mol), less energy is required for the six-membered ring TS2 (108.6 kcal/mol) to fracture and produce levoglucosan (Fig. 3e). Specifically, the hydroxyl groups on the surface of MXene interact with the hydroxyl group at position 6 and the oxygen atom at position 1 in cellulose through hydrogen bonding, forming the six-membered ring TS. Subsequently, the hydroxyl group at position 6 donates a proton to MXene and forms a bond with the carbon atom at position 1. At the same time, the proton on the hydroxyl group of MXene is transferred to the oxygen atom at position 1, leading to the breaking of the carbon-oxygen bond at position 1 (Figs. 3f1 and f2). As a result, the reaction causes the dissociation of cellulose into levoglucosan and glucopyranose. Consequently, the presence of MXene as a catalyst significantly enhances the likelihood of levoglucosan formation from cellulose.

In order to obtain more accurate and reliable experimental results, better simulate industrial production conditions, and more convenient separation and recycle of MXene catalyst, laboratory-scale biomass pyrolysis experiments were conducted in fixed bed setup with the pyrolysis temperature set at 540 °C. The influence of MXene-to-biomass ratios on levoglucosan yield was investigated and the mass balance of products is showcased in Fig. 4a. In comparison to Py-GC/MS analysis, the production of levoglucosan was considerably lower due to the slower heating rate and longer thermal treatment duration. As the catalyst-to-biomass ratio shifted from 20 wt% to 30 wt%, the yield of levoglucosan showed a significant upward trend, increasing from 6.12 wt% to 13.35 wt%. Subse-

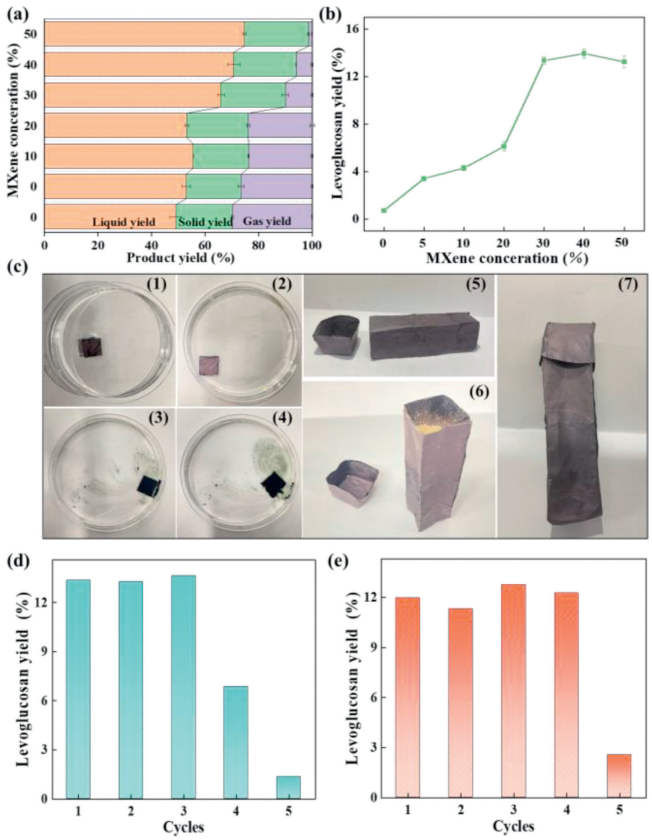

Fig. 4. (a) Mass balance of experimental cases performed with MXene (P); (b) Levoglucosan yield with different ratios of MXene (P); (c) Fabrication of welded MXene (Box). Note: In Fig. c, (1), (2), (3), (4) represent the water tolerance of a fresh MXene film tested by manual shaking, while (5), (6), (7) depict the MXene box with biomass. (d) Levoglucosan yield in each recycling experiment with MXene (P). (e) Levoglucosan yield in each recycling experiment with MXene (Box_R).

quently, the levoglucosan yield plateaued at approximately 13 wt% with a catalyst ratio of 30 wt%, 40 wt%, and 50 wt%. Thus, the optimal addition of MXene was determined to be 30 wt% (Fig. 4b).

Drawing from our previous study [7], we discovered the phenomenon of water-assisted time-sensitive welding in MXene film. Possessing remarkable strength and flexibility, the MXene film can be easily shaped into various forms. Thus, we create a 3D box capable of containing biomass during the pyrolysis process (Fig. 4c). For this MXene (Box), the amount of MXene catalyst was maintained at approximately 0.3 g (30 wt% of the biomass) with 1 g of biomass inside. The levoglucosan yield for this MXene (Box) catalyst was around 12 wt%, slightly lower than that of the MXene (P) catalyst with the same ratio. This can be attributed to the relatively smaller effective contact area between MXene (Box) and biomass compared to MXene (P).

To explore the potential and feasibility of utilizing MXene catalyst for levoglucosan production on a commercial scale, recycling experiments were conducted using MXene (P_R) and MXene (Box_R) over five consecutive runs without regenerating the recycled MXene catalyst. The results are presented in Figs. 4d and e which were obtained at a MXene (P_R)/MXene (Box_R)-to-biomass ratio of 30 wt% and a temperature of 540 °C. Fig. 4d shows a slight decrease in levoglucosan yield after the first recovery of the MXene catalyst. However, after the third run of MXene (P_R), the levoglucosan yield remained around 13.5 wt%, demonstrating good stability. Similarly, MXene (Box_R) exhibited persistent catalytic efficacy after undergoing four consecutive cycles (Fig. 4e). It is important to highlight that the catalytic efficacy of MXene (Box_R) diminished notably after the fourth round of pyrolysis recycling. However, for MXene (Box_R) by the fourth recycling, the box easily fragmented, and by the fifth recycle test, complete fragmentation occurred, rendering further recycling impractical. This phenomenon primarily arises from the susceptibility of $Ti_3C_2T_x$ to oxidation by both oxygen and water molecules. The oxidation process is accelerated, particularly at high temperatures. The limited high-temperature tolerance of $Ti_3C_2T_x$ hinders its industrial application. Subsequent research endeavors will prioritize the enhancement of its antioxidant properties.

In conclusion, we present a pioneering study on the use of MXene, in thermocatalytic biomass pyrolysis for levoglucosan production. Our findings remarkably demonstrate that incorporating MXene leads to a substantial increase in levoglucosan yield, effectively suppressing the formation of competing compounds. This significant contribution not only sheds light on a new direction for catalyst selection in the field of two-dimensional materials but also establishes a simple and energy-efficient approach to enhance the production of platform chemicals derived from biomass.

Declaration of completing interests

The authors declare that they have no known competing financial interests or personal relationships that could have appeared to influence the work reported in this paper.

Acknowledgment

The authors are grateful for the financial support provided by the National Natural Science Foundation of China (Nos. 22108221 and 52203145).

References

[1] J.L. Zheng, Y.H. Zhu, M.Q. Zhu, G.T. Sun, R.C. Sun, Green Chem. 20 (2018) 3287–3301.
[2] T.A. Werpy, G.E. Petersen, A. Aden, et al., TN, USA: U.S. Department of Energy, 76 (2004) 9–26.
[3] I. Itabaiana Jr., M.A. do Nascimento, R.O.M.A. de Souza, A. Dufour, R. Wojcieszak, Green Chem. 22 (2020) 5859–5880.
[4] H. Bhattarai, E. Saikawa, X. Wan, et al., Atmos Res. 220 (2019) 20–33.
[5] X.W. Yang, A.Q. Zheng, Z.L. Zhao, et al., Ind. Crops Prod. 168 (2021) 13.
[6] L.Q. Jiang, Y.X. Wu, Z.L. Zhao, et al., Cellulose 26 (2019) 7877–7887.
[7] J.F. Wang, Y.Y. Liu, Y.Q. Yang, et al., Matter 5 (2022) 1042–1055.
[8] Y.Y. Yang, Y.Q. Xu, Q.H. Li, Y.G. Zhang, H. Zhou, J. Mater. Chem. A 10 (2022) 19444–19465.
[9] M. Alhabeb, K. Maleski, B. Anasori, et al., Chem. Mater. 29 (2017) 7633–7644.
[10] L.Q. Jiang, A.Q. Zheng, J.G. Meng, et al., Bioresour. Technol. 274 (2019) 281–286.
[11] M. Wang, S. Zhang, X.J. Liu, Y.Y. Ma, J.Q. Wang, Ind. Crops Prod. 201 (2023) 8.
[12] E. Leng, Y. Wang, X. Gong, et al., Proc. Combust. Inst. 36 (2017) 2263–2270.
[13] G.J. Kwon, D.Y. Kim, S. Kimura, S. Kuga, J. Anal. Appl. Pyrolysis 80 (2007) 1–5.
[14] X. Yang, Z. Fu, D. Han, et al., Renew Energy 147 (2020) 1120–1130.